Chapter 11
Other Field-Assisted Sintering Techniques

A number of sintering methods use electromagnetic radiation to rapidly heat the powder samples. The character and mechanisms of interaction of electromagnetic waves with materials depend on the wavelength of radiation. Microwave sintering has been discussed in Chap. 7. Other types of radiation can also be used to deliver energy to particle assemblies and induce inter-particle sintering. Infrared (IR) radiation is one of the means of energy transfer in furnaces. Recently, IR radiation-producing modules have been designed allowing for rapid heating and sintering of powder layers into films. IR radiation can also be produced by lasers and is constantly produced by the sun. Metallic particles meeting certain size requirements can be heated by intense light from a xenon lamp, while ultraviolet (UV) radiation can assist in conducting chemical reactions that facilitate sintering. In this chapter, principles and possibilities of powder sintering using IR radiation emitted by specially designed modules and laser-assisted, solar, photonic, and ultraviolet sintering are briefly discussed.

11.1 IR Radiation-Assisted Sintering

This section describes sintering assisted by IR radiation produced by specially designed modules. In the manufacturing of flexible electronics, conventional sintering limits the feasibility of the roll-to-roll processing [1] due to long times required for sintering. Sowade et al. [2] reported IR radiation drying and sintering of inkjet-printed silver layers on a nonabsorbent polyethylene naphthalate substrate. Drying and sintering were conducted using an IR module equipped with tube emitters made of quartz glass (Fig. 11.1). Each emitter consisted of two tungsten filaments. A U-shaped aluminum reflector was placed above the tube emitters to increase the efficiency of the IR system. Another reflector was installed under the substrate to intensify the IR irradiation due to reflection. At a higher filament

E. A. Olevsky, D. V. Dudina, *Field-Assisted Sintering*,
https://doi.org/10.1007/978-3-319-76032-2_11

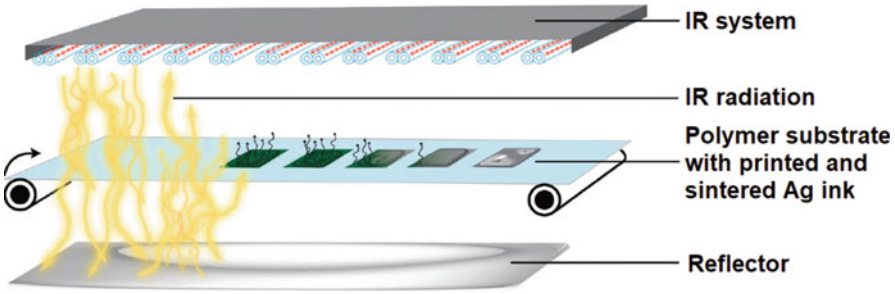

Fig. 11.1 IR radiation module for sintering of inkjet-printed layers of silver on a polymer substrate. (Reproduced from Ref. [2] with permission of The Royal Society of Chemistry)

temperature, drying and sintering was more efficient, as the silver layer has a higher absorbance in the shorter wavelength range.

Georgiadis et al. [3] emphasized the benefit of IR radiation heating over convection and conduction, which lies in the energy efficiency. They reported the formation of smooth and crack-free films from a hard latex using IR radiation sintering of dried layers deposited from emulsion. Using IR radiation-assisted sintering, the film could be obtained without adding plasticizers, which is a great benefit over the conventional processing, as during the film formation, plasticizers cause the evolution of volatile organic compounds – substances harmful from the environmental and health standpoints. In order to assist absorption of the IR radiation by the film, an additive – a near-IR-absorbing polymer – was used at a concentration of 1 wt.%. The non-sintered film consisted of spherical particles with voids between them (Fig. 11.2a). After treatment under a 250 W near-IR lamp for 4 min, the particles flattened, and the size of the voids decreased (Fig. 11.2b). After 30 min of treatment (Fig. 11.2c), the separate particles were more difficult to distinguish, which indicated sintering. The particle flattening was quantitatively analyzed by measuring the topographic profiles of the films after IR radiation-assisted sintering and heating in an oven. Figure 11.3 shows the dependence of the peak-to-valley height of the films on the time of exposure making it obvious that direct IR treatment of the films leads to a more rapid flattening (and sintering) of the particles in comparison with conventional treatment in an oven.

11.2 Solar Sintering

Solar radiation is a powerful and ecological energy source. A series of recent laboratory studies have been conducted using a solar furnace of the Plataforma Solar de Almería, Spain [4]. This solar furnace consists of the following elements: a continuous solar-tracking flat heliostat, a parabolic concentrator mirror (collector), an attenuator (shutter), and a test zone located in the concentrator focus center (Fig. 11.4). The shutter is used to regulate the amount of the incident light. When

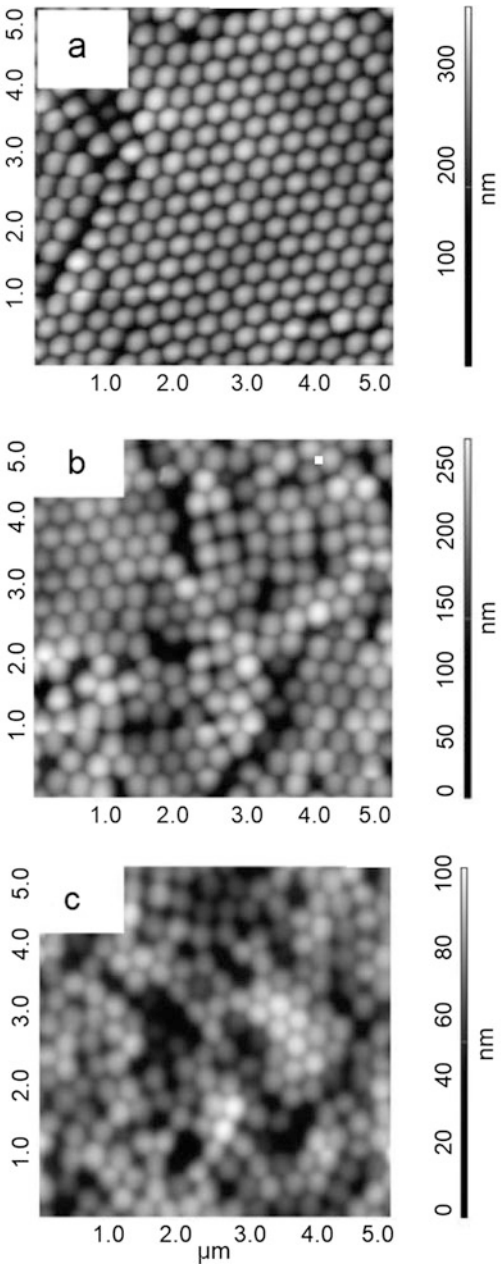

Fig. 11.2 Atomic force microscopy height images of the latex films deposited at room temperature (**a**), after 4 min (**b**), and 30 min (**c**) of IR radiation treatment. The images size is 5 μm × 5 μm. (Reprinted with permission from Georgiadis et al. [3]. Copyright (2011) American Chemical Society)

it is 100% open and the direct solar irradiance is 1000 $W \cdot m^{-2}$, the focus has an irradiance peak of 3051 $W \cdot m^{-2}$, a total power of 70 kW, and a focal diameter of 26 cm. A possibility of sintering of alumina at 1780 °C was reported [4]. Technical issues associated with solar furnaces include overshoot of temperature at the onset of

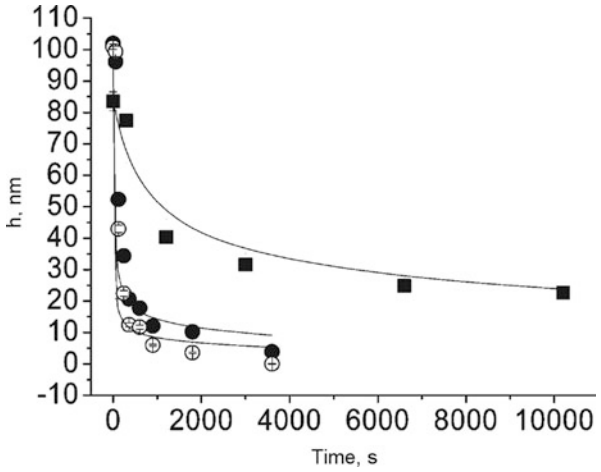

Fig. 11.3 Dependences of the peak-to-valley height on the time of continuous exposure to near-IR radiation for the acrylic additive-free latex (filled circles) and latex with 1 wt.% of IR-absorbing polymer (empty circles) and treatment in an oven at 60 °C (squares). Error bars span the size of the symbols. During the first 10 min in the oven, there was not significant sintering due to slow heating, so $t = 0$ corresponds to 10 min of holding. (Reprinted with permission from Georgiadis et al. [3]. Copyright (2011) American Chemical Society)

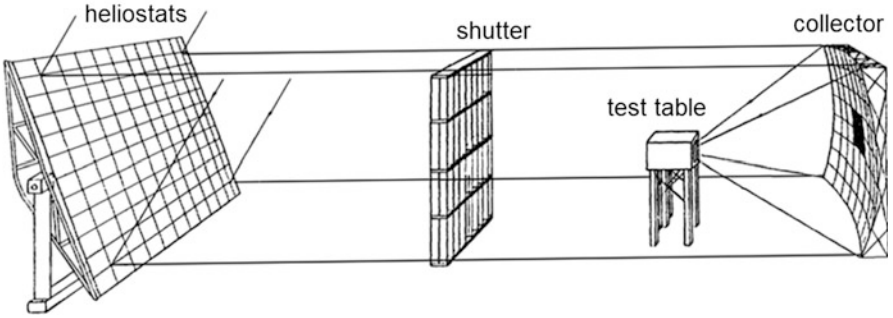

Fig. 11.4 Solar furnace of the Plataforma Solar de Almería, Spain. (Reprinted from Román et al. [4]. Copyright (2008), with permission from Elsevier)

solar heating and difficulties in the precise temperature control of the sintered part [5]. The temperature overshoot may result in the formation of a liquid phase and undesirable shape distortions. Due to large investment costs, solar sintering facilities are still expensive tools having a potential of cost reduction in the medium term [4].

A comparison between the microstructure of alumina consolidated by solar sintering and that of alumina sintered in an electric furnace was made (Fig. 11.5) [4]. The compacts were sintered by the two methods at the same maximum temperature of 1600 °C but with different heating rates and dwell times. The compact

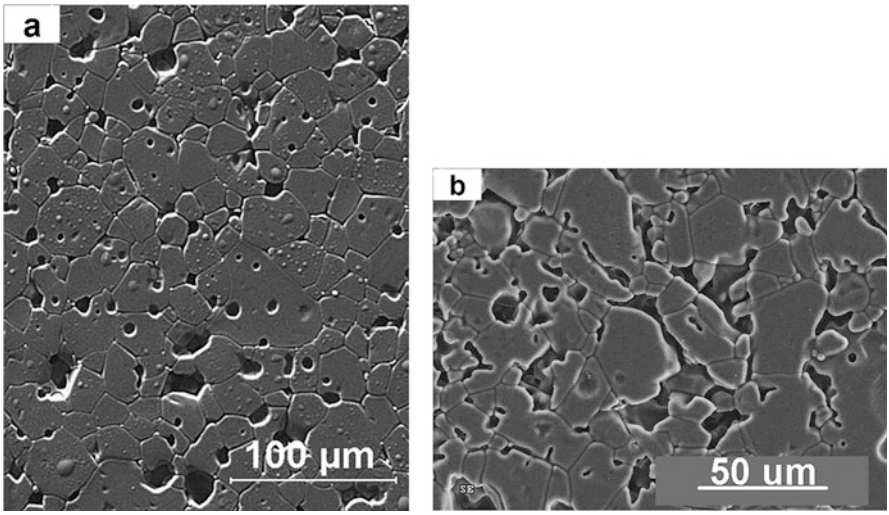

Fig. 11.5 Microstructure of alumina consolidated by solar sintering, heating rate 50 °C·min^{-1}, dwell time 60 min, relative density 95% (**a**), and sintered in a resistance furnace, heating rate 5 °C·min^{-1}, dwell time 240 min, relative density 89% (**b**). Maximum sintering temperature 1600 °C. (Reprinted from Román et al. [4]. Copyright (2008), with permission from Elsevier)

consolidated by solar sintering was denser than that sintered in a furnace (95% vs. 89% relative density). The degree of sintering was also reflected in the microstructure. The solar sintered compact had well-defined polygonal grains: the 300 nm particles of the powder experienced growth such that the compact consisted of grains as large as 20 µm. A significant number of voids of spherical shape are seen in the microstructure of the solar sintered material; these voids are located within the matrix grains (Fig. 11.5a). The voids were observed on a polished surface. However, using a different sample preparation technique, it was proved that these voids were initially (before polishing) filled with particles, which indicates incomplete sintering. In the compact sintered from the same powder in an electric furnace, only a few areas that experienced sintering could be found (Fig. 11.5b), the voids were located at grain boundaries, and the sintered material consisted of 50 µm grains. The microstructures of the compacts sintered by the two methods show that an improvement of densification was achieved by using solar sintering instead of sintering in a furnace. With the use of solar sintering, a significantly reduced duration of sintering was achieved for other materials: e.g., cordierite ceramics was sintered by solar sintering within 60 min, while in conventional sintering, about 24 h is needed for the process completion [5].

11.3 Laser-Assisted Sintering

Laser-assisted sintering is used for the fabrication of films in printed electronics and 3D objects. A detailed description of the interactions of laser radiation with materials and selective laser sintering is beyond the scope of this book and can be found in the literature on laser processing of materials [6] and 3D manufacturing [7–9]. The use of different types of lasers for different materials has been described by Lee et al. [10]. Selective laser sintering of metals is also referred to as direct metal laser sintering. In this process, Nd:YAG lasers (output wavelength 1064 nm) or Yb-fiber lasers (output wavelengths 1030–1070 nm) exhibit a higher throughput than CO_2 lasers with an operating wavelength of 10.6 μm. Nd:YAG and Yb-fiber lasers are also used for sintering of carbide ceramics. CO_2 lasers are suitable for sintering of polymers as the latter have high absorptivity at the operating wavelength of these lasers. Sintering of oxide ceramics is also possible with the use of CO_2 lasers.

In selective laser sintering, partial melting of the powder material can be achieved, and in this way, selective laser sintering bears similarities with electric current-assisted sintering, in which the inter-particle contacts in an electric current-carrying specimen can experience melting, while the particle volumes will continue to remain solid. Another similarity of electric current-assisted sintering and selective laser sintering is the dynamic nature of the processes, as the responses of the materials to the external field change with time. Normally, in the processes of electric current-assisted sintering, the contribution of inter-particle contacts to the total resistance of the sample decreases as sintering progresses due to the formation of well-established inter-particle contacts. At the same time, the resistivity of materials is a function of temperature and changes upon heating. During laser treatment, the absorptivity and thermal conductivity of the material are the important properties; these properties change with the temperature and the structure of the powder layer as the powder particles sinter between themselves [11, 12]. Absorption of laser radiation is favored by porosity of the powder layer and non-flat surfaces. Olakanmi et al. [8] indicate the relevance of the information on the sintering behavior of a powder during pulsed electric current-assisted sintering to selective laser sintering and suggest using the accumulated knowledge in the field of pulsed current sintering for gaining insights into the mechanisms of laser-assisted sintering.

11.4 Photonic Sintering

Sintering of nanoparticles using irradiation by light – photonic sintering in a continuous [13] or flash mode [14–22] – is attracting attention due to possibilities of fast processing of printed electronics and flexible dye-sensitized solar cells under ambient conditions as well as using large-area and temperature-sensitive substrate materials. In photonic sintering, films formed by nanoparticle inks or pastes are

heated by irradiation. The method uses the differences in the absorption properties of the substrate and the film composed of nanoparticles. The solvent is evaporated and sintering between the nanoparticles occurs. By choosing radiation with a desired emission spectrum, energy can be "pumped" selectively into the printed ink structures without directly affecting the substrate. As the electromagnetic radiation directly affects the printed structures and not the film/substrate system as a whole, sintering is accelerated compared with the conventional process of heating in an oven.

Photonic sintering is conducted without the application of pressure making temperature the key factor influencing the film densification [23]. Govorov and Richardson [24] analyzed the generation of heat in metal nanoparticles irradiated by light. Heating is strongly enhanced under the conditions of the plasmon resonance. It was found that the temperature increase of the nanoparticles $\Delta T_{\max}$ is proportional to the second power of the nanoparticle radius R_{np}:

$$\Delta T_{\max} \propto R_{\mathrm{np}}^2$$

This size dependence of the temperature increase is governed by the total rate of heat generation and by heat transfer through the nanoparticle surface. The heating process also depends on the shape and organization of nanoparticles due to collective effects.

The results of photonic sintering depend on the size of metallic nanoparticles. Park and Kim [19] studied flash light sintering of nickel nanoparticles and found that while particles with a broad size distribution (5–500 nm) were successfully sintered by the flash light irradiation (xenon lamp, wavelengths 380 nm–1 μm), the films consisting of 50 nm particles were poorly sintered. The sheet resistance of the sintered films decreased with increasing sintering energy, which indicates the progress of sintering. The sheet resistance of the films obtained from the 50 nm particles was 2–3 orders of magnitude greater than that of the films obtained from the ink containing nickel nanoparticles with a broad size distribution. Better sinterability of the films obtained from the ink containing 5–500 nm nickel particles was explained by a better absorption of light (absorption of light with a wide range of wavelengths) by particles of different sizes, as shown in Fig. 11.6, and the presence of very fine nanoparticles, whose melting temperatures are much lower than that of bulk nickel. Early melting of very fine particles was suggested as a crucial step in flash light sintering, as the molten material can connect larger particles and facilitate the sintering process as a whole.

Park and Kim [19] utilized preheating before the main sintering step to improve the quality of the sintered films. As can be seen from images of the films sintered at 17.5 J·cm^{-2} at the main sintering step, the film preheated at 12.5 J·cm^{-2} had a more densely connected necking structure (Fig. 11.7a) than the film preheated at 7.5 J·cm^{-2} (Fig. 11.7b).

MacNeill et al. [13] analyzed photonic sintering of silver nanoparticles both experimentally and theoretically and found that it is an inherently self-damping process. The progress of densification reduces the magnitude of subsequent photonic

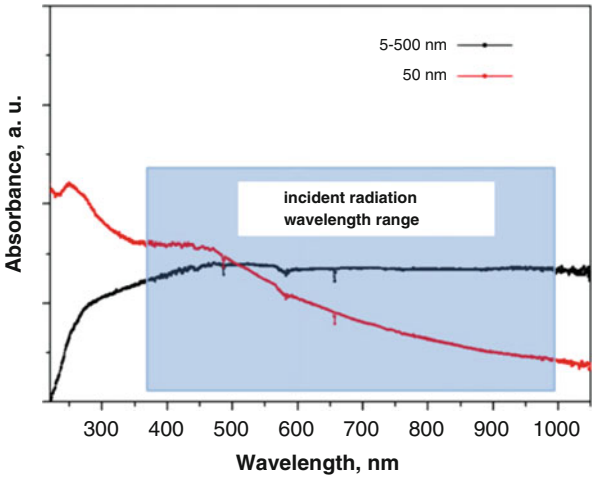

Fig. 11.6 Absorbance of light by nickel nanoparticles with different sizes and size distributions. (Reprinted from Park et al. [19]. Copyright (2013), with permission from Elsevier)

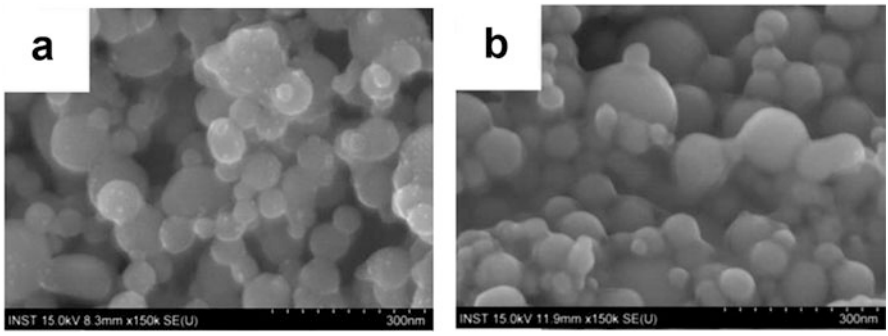

Fig. 11.7 Morphology of the films obtained from nickel nanoparticles 5–500 nm in size: (**a**) preheating at 12.5 J·cm^{-2}, (**b**) 7.5 J·cm^{-2} (the main sintering step at 17.5 J·cm^{-2}). (Reprinted from Park and Kim [19]. Copyright (2013), with permission from Elsevier)

heating. Bansal and Malhotra [23] measured the temperature of the silver nanoparticle films during their sintering by intense pulsed light. Measurements were done using a thermal camera. Under high fluencies, a turning point in the evolution of the film temperature during sintering was observed: with increasing the number of pulses, the temperature dropped down after the initial rise. The film densification leveled off beyond a critical pulse fluence and a critical number of pulses. A computational model that is able to capture the experimentally observed turning point in the temperature during sintering was developed. This model links the electromagnetic finite element analysis of optical energy absorption and semi-analytical models of inter-particle neck growth to mesoscale transient heat transfer and densification of the films. It was found that the temperature turning occurs due to a coupling between optical absorption and densification in the nanoparticle film: a reduction of optical absorption was caused by the inter-particle neck growth and changes in the particle shape.

11.5 UV-Assisted Sintering

UV radiation is useful in the processes that require conducting chemical reactions along with particle sintering. UV light was used by Oh et al. [25] to sinter TiO_2 nanoparticles for the fabrication of dye-sensitized solar cells. An organic compound-containing titanium was introduced into the TiO_2-based ink. This compound decomposed under UV radiation forming TiO_2 particles, which bonded the pre-existing TiO_2 particles together. In a study by Hwang et al. [26], deep UV light caused decomposition of a poly(N-vinylpyrrolidone) coating on copper nanoparticles so that the oxide shells on the particles were efficiently reduced.

11.6 Selected Examples of Materials Obtained Using Infrared, Solar, and Photonic Sintering

IR radiation-assisted sintering has been used for nanoparticles of metals [2], polymers [3], and oxides [27]. A limiting step to the roll-to-roll production of dye-sensitized solar cells on metals is sintering of nanoparticles of TiO_2. Watson et al. [27] suggested a near-IR heating method, in which titanium substrates are heated directly causing the removal of the binder and sintering of the TiO_2 particles. Sintering of the same assemblies in a conventional oven at temperatures close to those achieved by IR heating and for much longer time yielded cell efficiencies equal to or lower than those manufactured by using IR heating.

Solar sintering is suitable for consolidating metals [28] and ceramic materials [4, 5, 29, 30] as well as metal–ceramic composites [31]. Rosa et al. [31] showed that WC–10wt.%Co materials with properties comparable to those of the conventionally processed cemented carbides can be obtained by fast solar sintering. The differences in the heating schedule in these two processes can be seen in Fig. 11.8, from which it follows that solar sintering allowed reaching a significant reduction of the sintering time. As hardness of the solar sintered WC–10 wt.% Co materials was as high as that of the conventionally processed cemented carbide (13 GPa) and the fracture toughness was 12 $MPa \cdot m^{1/2}$, which is only 10% lower than the value of the fracture toughness of the conventionally processed cemented carbide, solar sintering was recommended as a cost-effective and environmentally friendly sintering method of cemented carbides. Close levels of hardness and fracture toughness could be expected from the similarity of the microstructures of these two materials (Fig. 11.9).

Photonic sintering was shown to be suitable for sintering of layers composed of metals [14–20], metal-containing composites [32], as well as conducting oxides [22] and semiconductors [21, 22]. Using photonic flash sintering, current collecting grids for solar cell applications were obtained starting from a silver nanoparticle ink, and the sintering results were compared with those produced by thermal treatment of the printed structures [20]. Grids obtained by photonic sintering

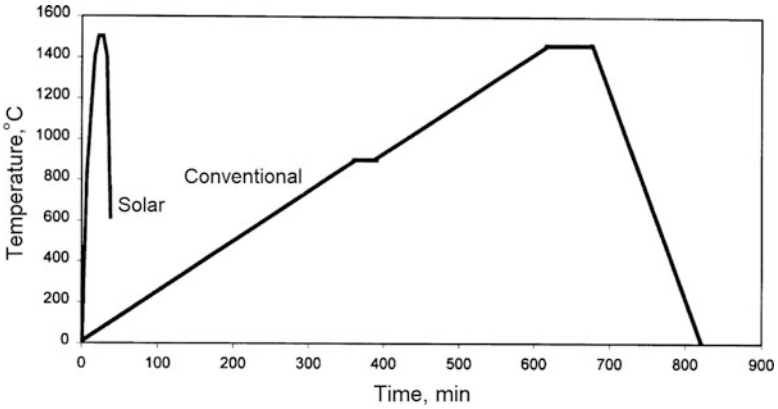

Fig. 11.8 Heating schedules in solar and conventional sintering of WC–10wt.%Co. (Reprinted from Rosa et al. [31]. Copyright (2002), with permission from Elsevier)

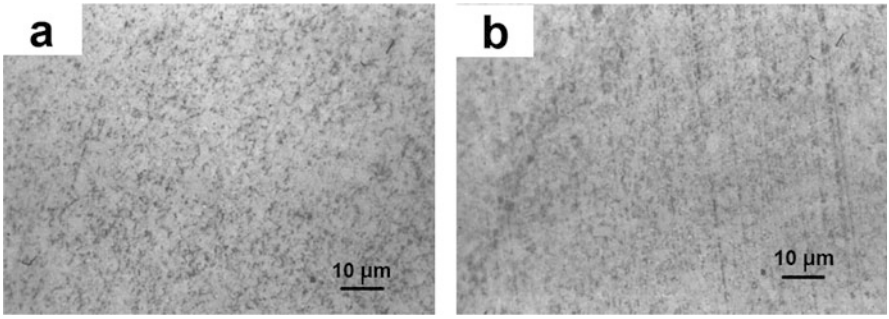

Fig. 11.9 Microstructure of solar (**a**) and conventionally sintered (**b**) WC–10wt.%Co. (Reprinted from Rosa et al. [31]. Copyright (2002), with permission from Elsevier)

exhibited advantages over thermally sintered ones in terms of geometry and conductivity. Worth mentioning are similar conductivities obtained after 5 s of photonic flash sintering and 6 h of thermal sintering. While a large number of studies on the feasibility of radiation-assisted methods of sintering of printed electronics have been published, direct assessment of different electromagnetic wave-assisted methods using the same object is rarely conducted. From a practical perspective, worth particular attention is study by Niittynen et al. [17], who compared the structure and properties of inkjet-printed samples of silver dispersion on polymer substrates sintered by different techniques – sintering in a convection oven (thermal sintering) and plasma, laser, and photonic sintering – and concluded on a better suitability of photonic sintering realized using a xenon flash lamp with an emission spectrum of 350–900 nm for scalable processing of films with good adhesion, high electrical conductivity, and a uniform and dense nanostructure. The temperature during photonic sintering could be high enough to cause substrate damage due to dissipation of heat from the metallic structure. The authors emphasized the importance of

tuning the pulse length, intensity, as well as sintering time to bring substrate damage to a minimum. An advantage of selectivity of sintering enabled by the laser sintering technique due to digital control was also highlighted.

Intense pulsed light can be used to initiate chemical reactions. In this regard, photonic treatment of printed CuO accompanied by its reduction to Cu_2O and further to metallic copper presents a viable route to the fabrication of elements of printed electronics [33]. Reduction of CuO nanoparticles contained in the ink was due to a process of photoreduction as well as the presence of reducing agents in the ink. Morphological transformations from the isolated copper nanoparticles to fully sintered Cu films could be controlled by changing the light intensity.

Joo et al. [34] tested the sintering behavior of films deposited from inks containing both copper nano- and microparticles. The resistivity of the film sintered from the microparticle ink (246 μΩ·cm) was greater than that of film obtained from the nanoparticle ink (210 μΩ·cm); these films were sintered under the same flash light sintering conditions. An interesting result was a lower resistivity of the film obtained from the ink containing both nano- and microparticles in the 50:50 volume ratio (80 μΩ·cm). The authors saw the reason for an advantage of inks with particles of mixed sizes in the capability of the nanoparticles to fill the pores between the microparticles. In the film fabricated from the nanoparticle ink, nanopores remained, while in the film sintered from the microparticles, the remaining pores had sizes comparable to the size of the microparticles. The problem of residual pores was successfully solved by a proper choice of the composition of the initial ink in terms of the size of nanoparticles. In order to increase the relative density of the flash light sintered films obtained from copper nanoparticle inks, Chung et al. [35] suggested adding copper-containing precursors that undergo chemical transformations resulting in the in situ formation of copper during flash light treatment of the films. Following this strategy, films with a low resistivity (27.3 μΩ·cm) were obtained from a mixed ink with copper (II) nitrate trihydrate as a copper-containing precursor.

In addition to single metal features, alloys and composite films can be obtained by radiation-assisted sintering. Zhao et al. [36] sintered copper features by using a pulsed green light laser and a pulsed UV laser and, in order to increase the resistance of copper to oxidation, suggested alloying it with gold. Alloying was also beneficial in reducing the melting point of the material. The Cu_xAu_{100-x} alloys when printed and laser-sintered can be used as a basis for flexible chemical sensors for the detection of environmental pollutants and breath biomarkers. Composite films consisting of copper and multiwalled carbon nanotubes were obtained by flash light sintering [32]. For that, carbon nanotubes were dispersed in the copper nanoparticle ink. In the films containing the same concentration of nanotubes, the size of the pores decreased with increasing nanotube length. The presence of carbon nanotubes improved the environmental stability of the films by slowing down the process of oxidation of copper to Cu_2O.

In addition to sintering of nanoparticles, welding of nanowires can occur under flash light treatment [37–39]. In order to improve the optical efficiency of a flash lamp and light absorbing yield, silver nanowires deposited on a substrate were encapsulated by a graphene layer [38]. In the presence of graphene, ultrafast welding

of the nanowires (in less than 20 ms) was observed under the intense pulsed light treatment, while pristine (uncoated) nanowires remained intact. The graphene layer is thought to effectively absorb the energy of radiation and transfer it to the silver nanowires. Mixed inks containing copper nanoparticles and copper nanowires in various proportions were tested by subjecting them to sintering under the same conditions [39]. The film flash light sintered from the ink with 5 wt.% of copper nanowires had a lower resistivity (22.77 μΩ·cm) than those obtained from the inks containing copper nanoparticles or nanowires only (94.01 μΩ·cm and 104.15 μΩ·cm, respectively).

Intense white light-assisted sintering was shown to be suitable for sintering of TiO_2 photoelectrodes [21]. The heating of the TiO_2 layer on tin-doped indium oxide-polyethylene terephthalate substrates was suggested to be caused by the sub-band absorption. The treatment of the TiO_2 film with intense pulsed light helped achieve interconnection between the TiO_2 particles and led an increase in the mechanical stability of the photoelectrode and an improvement of the power conversion efficiency over the entire spectral range.

11.7 Summary

This chapter reviewed the principles of sintering techniques based on the application of electromagnetic radiation to powder materials – IR radiation-assisted, laser, solar, photonic, and UV sintering. To enable rapid heating and sintering of powders, IR radiation-producing modules have been designed. IR radiation can also be generated by lasers and is contained in the solar radiation spectrum. Laser sintering is widely used in the layer-by-layer 3D manufacturing of parts from metallic, ceramic, and polymer materials. Solar energy is a clean and ecological type of energy. However, it requires large initial investments into the facilities. Solar sintering is suitable for metals, ceramics, and composite materials and offers faster heating and more rapid densification than conventional furnace sintering. Photonic sintering is conducted mainly by intense pulsed light radiation in the 380 nm–1 μm wavelength range. It is suitable for sintering of metallic nanoparticles, metal-containing composites, as well as semiconductors. A growing interest to IR radiation-assisted and photonic sintering is due to their compatibility with the roll-to-roll fabrication of flexible electronics. UV light is instrumental in initiating chemical reactions and can be used to facilitate sintering when the products of the in situ conducted reactions have advantages in terms of composition and particle size for the progress of sintering. For almost all of the mentioned sintering techniques, the published studies are predominantly descriptive and provide mainly qualitative analyses. An in-depth consideration of these sintering approaches' underlying physical phenomena and the related predictive modeling represent the future research directions.

References

1. Morrison NA (2016) Roll-to-roll processing of flexible devices and components: utilization in wearable and mobile electronics and the coming IOT era. Vakuum in Forschung und Praxis 28 (4):30–35
2. Sowade E, Kang H, Mitra KY, Weiß OJ, Weber J, Baumann RR (2015) Roll-to-roll infrared (IR) drying and sintering of an inkjet-printed silver nanoparticle ink within 1 second. J Mater Chem C 3:11815–11826
3. Georgiadis A, Bryant PA, Murray M, Beharrell P, Keddie JL (2011) Resolving the film-formation dilemma with infrared radiation-assisted sintering. Langmuir 27:2176–2180
4. Román R, Cañadas I, Rodríguez J, Hernández MT, González M (2017) Solar sintering of alumina ceramics: microstructural development. Sol Energy 82:893–902
5. Oliveira FAC, Rosa LG, Fernandes JC, Rodríguez J, Cañadas I, Martínez D, Shohoji N (2009) Mechanical properties of dense cordierite discs sintered by solar radiation heating. Mater Trans 50:2221–2228
6. Gladush GG, Smurov I (2011) Physics of laser materials processing: theory and experiment, Springer Series in Materials Science (SSMATERIALS, V. 146), USA, 534 p
7. Gibson I, Rosen DW (2015) Stucker B (2010) additive manufacturing technologies: 3D printing, rapid prototyping, and direct digital manufacturing, 2nd edn. Springer Science+Business Media, New York, 498 p
8. Olakanmi EO, Cochrane RF, Dalgarno KW (2015) A review on selective laser sintering/melting (SLS/SLM) of aluminium alloy powders: processing, microstructure, and properties. Prog Mater Sci 74:401–477
9. Shishkovsky I, Yadroitsev I, Bertrand P, Smurov I (2007) Alumina–zirconium ceramics synthesis by selective laser sintering/melting. Appl Surf Sci 254(4):966–970
10. Lee H, Huat Joel Lim C, Ji Low M, Tham N, Matham Murukeshan V, Kim YJ (2017) Lasers in additive manufacturing: a review. Int J Prec Eng Manuf Green Technol 4(3):307–322
11. West C, Wang X (2017) Modeling of selective laser sintering/selective laser melting. In: Gu B, Helvajian H, Piqué A, Dunsky CM, Liu J (eds) Laser 3D manufacturing IV. Proc SPIE 10095, USA, p 1009506
12. Boley CD, Khairallah SA, Rubenchik AM (2014) Calculation of laser absorption by metal powders in additive manufacturing. LLNL-JRNL-665313, USA
13. MacNeill W, Choi CH, Chang CH, Malhotra R (2015) On the self-damping nature of densification in photonic sintering of nanoparticles. Sci Rep 5:14845
14. Kim HS, Dhage SR, Shim DE, Hahn HT (2009) Intense pulsed light sintering of copper nanoink for printed electronics. Appl Phys A Mater Sci Process 97:791–798
15. Hwang HJ, Chung WH, Kim HS (2012) In situ monitoring of flash-light sintering of copper nanoparticle ink for printed electronics. Nanotechnology 23:485205
16. Hösel M, Krebs FC (2012) Large-scale roll-to-roll photonic sintering of flexo printed silver nanoparticle electrodes. J Mater Chem 22:15683–15688
17. Niittynen J, Abbel R, Mäntysalo M, Perelaer J, Schubert US, Lupo D (2014) Alternative sintering methods compared to conventional thermal sintering for inkjet printed silver nanoparticle ink. Thin Solid Films 556:452–459
18. Park SH, Chung WH, Kim HS (2014) Temperature changes of copper nanoparticle ink during flash light sintering. J Mater Proc Technol 214:2730–2738
19. Park SH, Kim HS (2014) Flash light sintering of nickel nanoparticles for printed electronics. Thin Solid Films 550:575–5811
20. Galagan Y, Coenen EWC, Abbel R, van Lammeren TJ, Sabik S, Barink M, Meinders ER, Andriessen R, Blom PWM (2013) Photonic sintering of inkjet printed current collecting grids for organic solar cell applications. Org Electron 14:38–46
21. Jin HY, Kim JY, Lee JA, Lee K, Yoo K, Lee DK, Kim B, Kim JY, Kim H, Son HJ, Kim J, Lim JA, Ko MJ (2014) Rapid sintering of TiO_2 photoelectrodes using intense pulsed white light for flexible dye-sensitized solar cells. Appl Phys Lett 104:1439027

22. Marjanovic N, Hammerschmidt J, Perelaer J, Farnsworth S, Rawson I, Kus M, Yenel E, Tilki S, Schubert US, Baumann RR (2011) Inkjet printing and low temperature sintering of CuO and CdS as functional electronic layers and Schottky diodes. J Mater Chem 21:13634–13639
23. Bansal S, Malhotra R (2016) Nanoscale-shape-mediated coupling between temperature and densification in intense pulsed light sintering. Nanotechnology 27(49):495602
24. Govorov AO, Richardson HH (2007) Generating heat with metal nanoparticles. NanoToday 2 (1):30–38
25. Oh Y, Lee SN, Kim HK, Kim J (2012) UV-assisted chemical sintering of inkjet-printed TiO_2 photoelectrodes for low-temperature flexible dye-sensitized solar cells. J Electrochem Soc 159: H777–H781
26. Hwang HJ, Oh KH, Kim HS (2016) All-photonic drying and sintering process via flash white light combined with deep-UV and near-infrared irradiation for highly conductive copper nano-ink. Sci Rep 6:19696
27. Watson T, Mabbett I, Wang H, Peter L, Worsley D (2011) Ultrafast near infrared sintering of TiO_2 layers on metal substrates for dye-sensitized solar cells. Prog Photovolt Res Appl 19 (4):482–486
28. Cañadas I, Martínez D, Rodríguez J, Gallardo JM (2004) Sintering of multilayered copper wires in a solar furnace. Proc. European Congress and Exhibition on Powder Metallurgy, The European Powder Metallurgy Association, UK
29. Oliveira FAC, Shohoji N, Fernandes JC, Rosa LG (2005) Solar sintering of cordierite-based ceramics at low temperatures. Sol Energy 78:351–361
30. Fernandes JC, Amaral PM, Rosa LG, Shohoji N (2000) Weibull statistical analysis of flexure breaking performance for alumina ceramic disks sintered by solar radiation heating. Ceram Int 26:203–206
31. Rosa LG, Amaral PM, Anjinho C, Fernandes JC, Shohoji N (2002) Fracture toughness of solar-sintered WC with Co additive. Ceram Int 28:345–348
32. Hwang HJ, Joo SJ, Kim HS (2015) Copper nanoparticle/multiwalled carbon nanotube composite films with high electrical conductivity and fatigue resistance fabricated via flash light sintering. ACS Appl Mater Interf 7:25413–25423
33. Paglia F, Vak D, van Embden J, Chesman ASR, Martucci A, Jasieniak JJ, Gaspera ED (2015) Photonic sintering of copper through the controlled reduction of printed CuO nanocrystals. ACS Appl Mater Interf 7:25473–25478
34. Joo SJ, Hwang HJ, Kim HS (2014) Highly conductive copper nano/microparticles ink via flash light sintering for printed electronics. Nanotechnology 252:656014
35. Chung WH, Hwang HJ, Kim HS (2015) Flash light sintered copper precursor/nanoparticle pattern with high electrical conductivity and low porosity for printed. Thin Solid Films 580:61–70
36. Zhao W, Rovere T, Weerawarne D, Osterhoudt G, Kang N, Joseph P, Luo J, Shim B, Poliks M, Zhong CJ (2015) Nanoalloy printed and pulse-laser sintered flexible sensor devices with enhanced stability and materials compatibility. ACS Nano 9(6):6168–6177
37. Mallikarjuna K, Hwang HJ, Chung WH, Kim HS (2016) Photonic welding of ultra-long copper nanowire network for flexible transparent electrodes using white flash light sintering. RSC Adv 6:4770–4779
38. Yang SB, Choi H, Lee DS, Choi CG, Choi SY, Kim ID (2015) Improved optical sintering efficiency at the contacts of silver nanowires encapsulated by a graphene layer. Small 11:1293–1300
39. Joo SJ, Park SH, Moon CJ, Kim HS (2015) A highly reliable copper nanowire/nanoparticle ink pattern with high conductivity on flexible substrate prepared via a flash light-sintering technique. ACS Appl Mater Interf 7:5674–5684